Supplement of Atmos. Chem. Phys., 25, 1333–1351, 2025
https://doi.org/10.5194/acp-25-1333-2025-supplement

Atmospheric Chemistry and Physics
Open Access
EGU

Supplement of

Impact of mineral dust on the global nitrate aerosol direct and indirect radiative effect

Alexandros Milousis et al.

Correspondence to: Vlassis A. Karydis (v.karydis@fz-juelich.de)

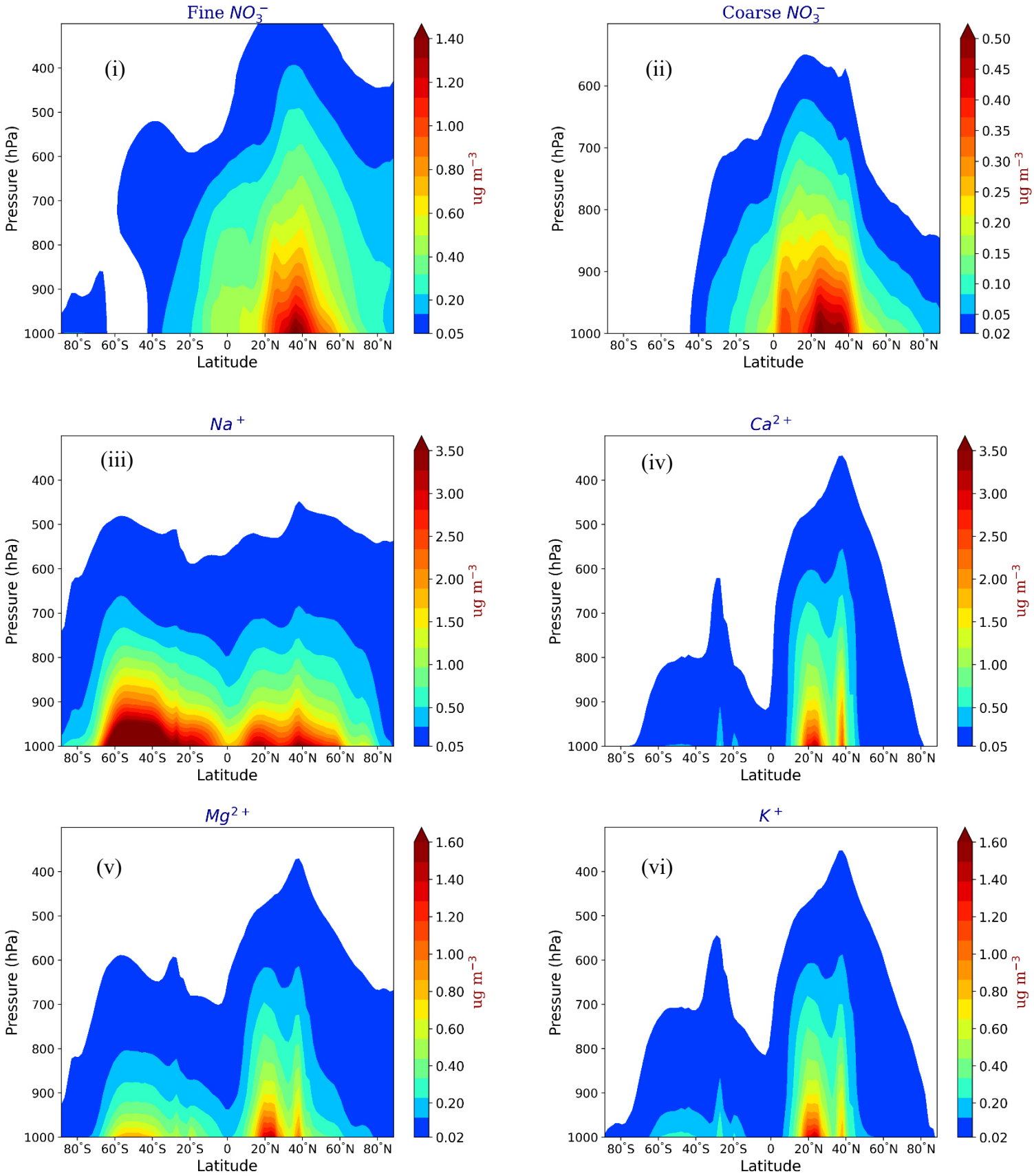

Figure S1 : Time averaged zonal concentrations of i) fine and ii) coarse aerosol NO_3^- , iii) Na^+ , iv) Ca^{2+}, v) Mg^{2+} and vi) K^+ in TSP as predicted by EMAC from the Base Case simulation.

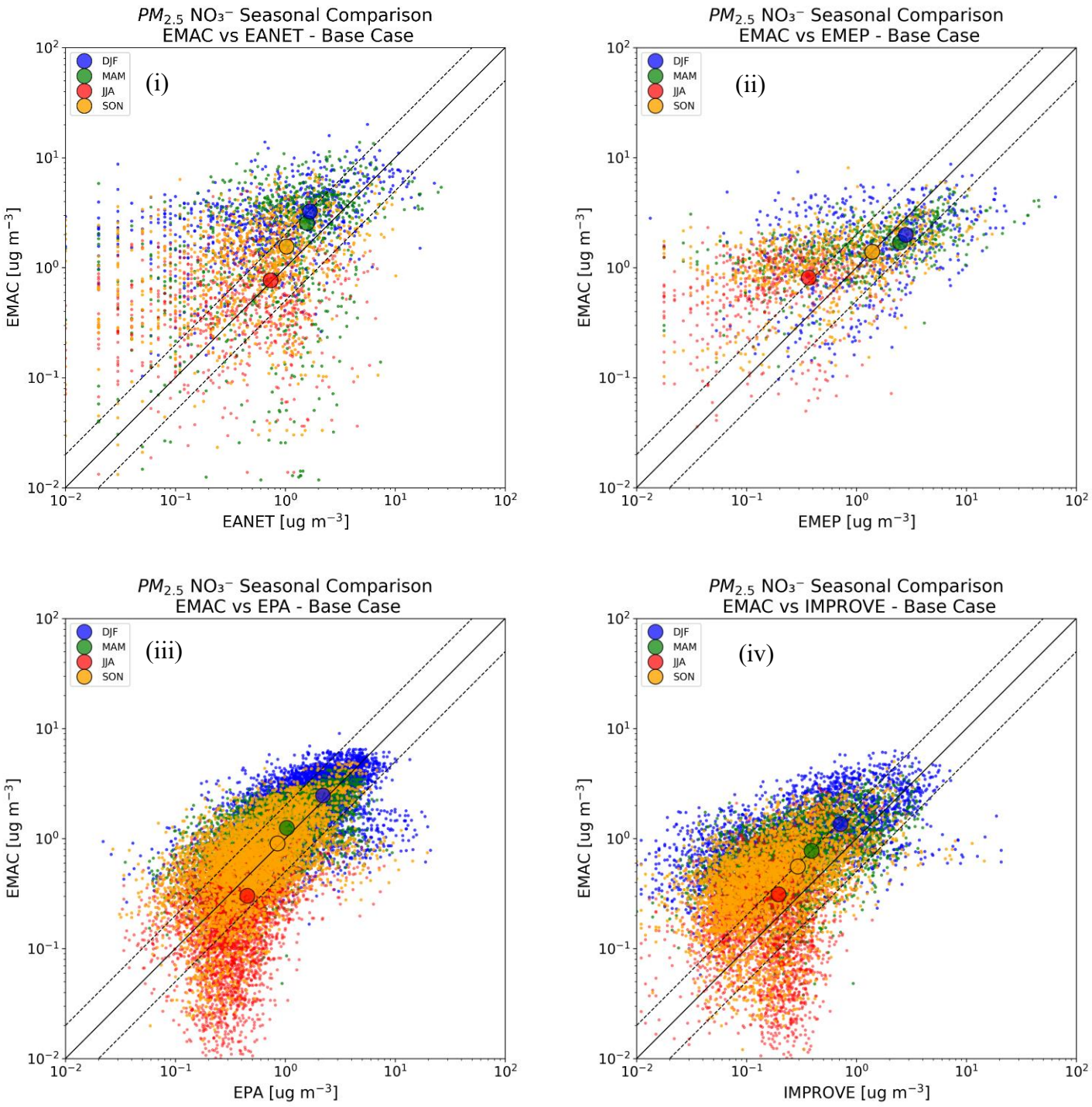

Figure S2: Scatterplots comparing the seasonal mean surface mass concentrations of $PM_{2.5}$ NO_3^- as simulated by EMAC from the Base Case simulation with observations from the networks of (i) EANET, (ii) EMEP, (iii) EPA and (iv) IMPROVE. Blue points indicate values in winter, green points in spring, red points in summer and yellow points in autumn. Enlarged dots indicate seasonal means. Also shown are the 1:1, 2:1, and 1:2 lines.

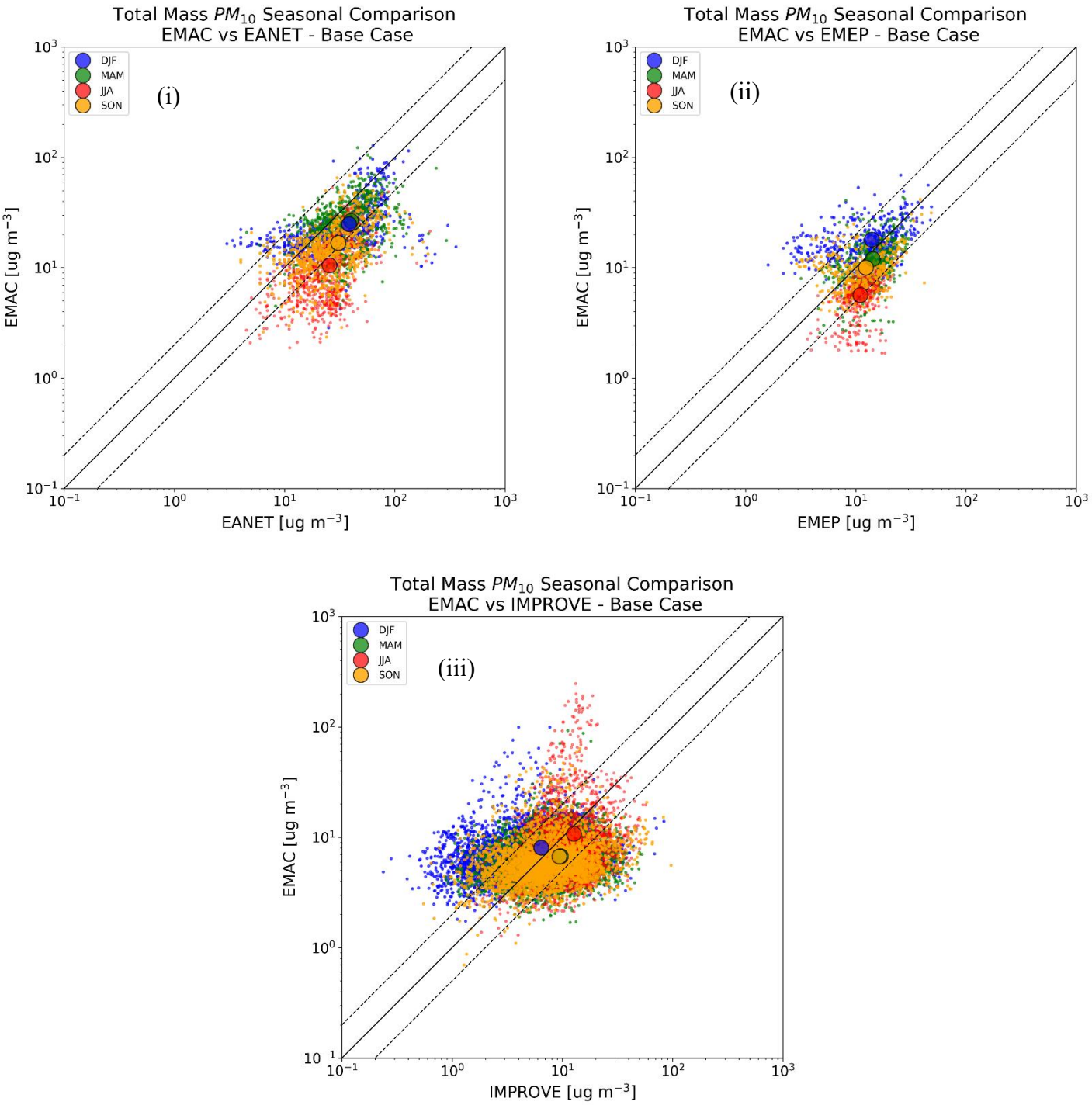

Figure S3: Scatterplots comparing the seasonal mean surface mass concentrations of PM_{10} aerosols as simulated by EMAC from the Base Case simulation with observations from the networks of (i) EANET, (ii) EMEP and (iii) IMPROVE. Blue points indicate values in winter, green points in spring, red points in summer and yellow points in autumn. Enlarged dots indicate seasonal means. Also shown are the 1:1, 2:1, and 1:2 lines.

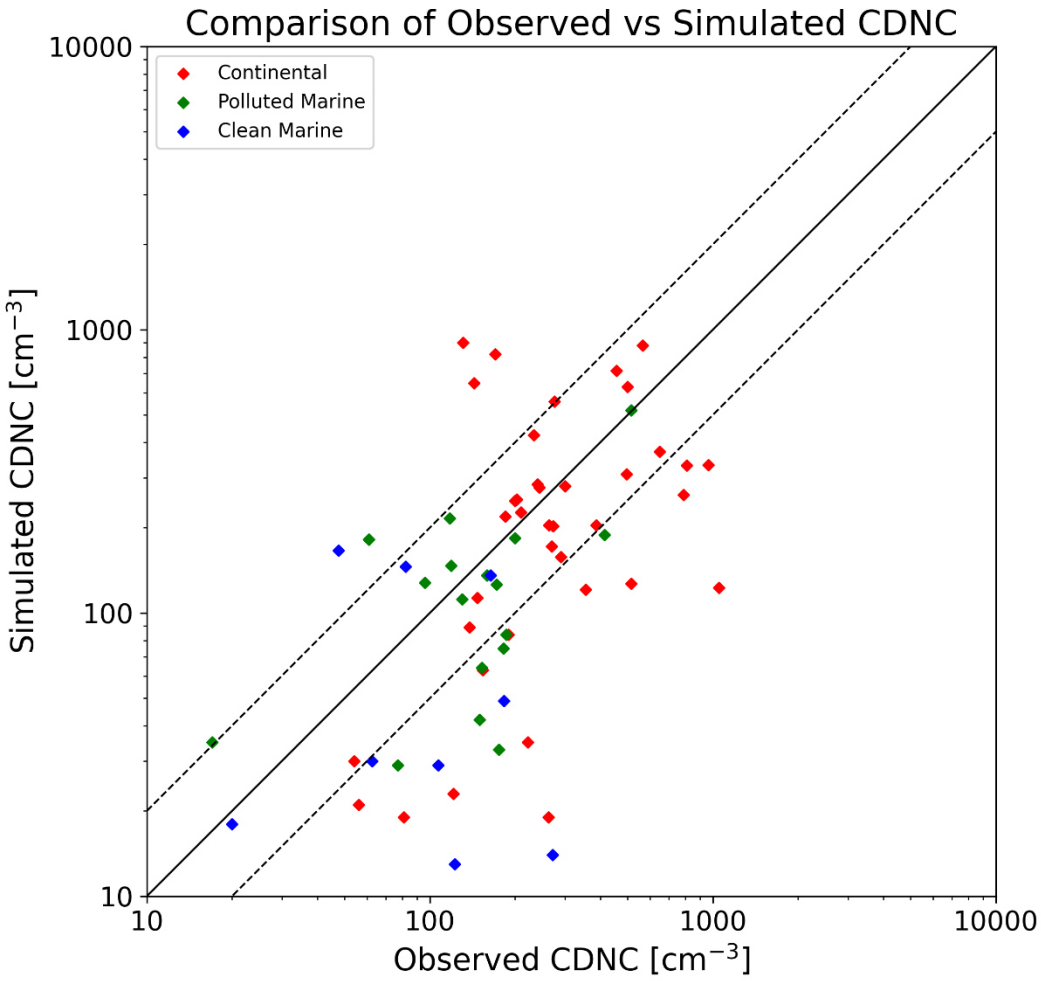

Figure S4: Comparison of global cloud droplet number concentrations as simulated by EMAC from the Base Case simulation and observed across different types of environments (continental, polluted and clean marine). The exact locations, altitudes and time periods of the measurements are shown in Table S3. Also shown are the 1:1, 2:1, and 1:2 lines.

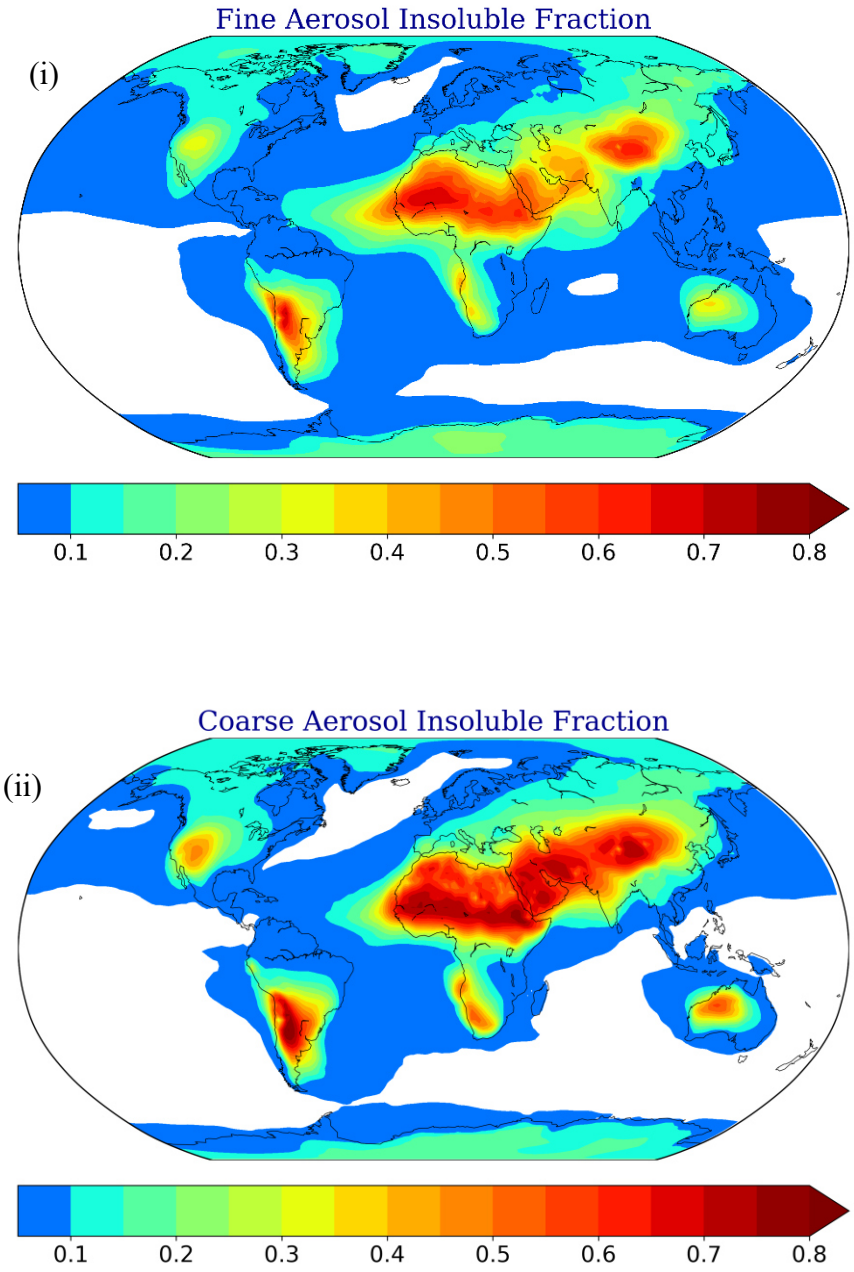

Figure S5 : Global mean insoluble fraction of (i) fine and (ii) coarse aerosols as predicted by EMAC from the Base Case simulation.

Table S1: Seasonal statistical evaluation of the EMAC predicted surface mass concentrations of $PM_{2.5}$ NO_3^- from the Base Case simulation against observations for the period 2008 - 2018.

Network	Season	Number of datasets	Mean Observed (μg m^{-3})	Mean Predicted (μg m^{-3})	MAGE (μg m^{-3})	MB (μg m^{-3})	NME (%)	NMB (%)	RMSE (μg m^{-3})
EPA	Winter	144	2.86	2.93	1.43	0.07	49.83	2.39	2.09
	Spring	291	1.63	1.78	0.71	0.14	43.54	8.84	1.09
	Summer	280	0.69	0.31	0.41	-0.38	59.5	-54.87	0.8
	Autumn	290	0.79	0.63	0.37	-0.16	46.88	-19.66	0.62
IMPROVE	Winter	116	0.92	1.52	1.03	0.6	111.16	64.6	1.48
	Spring	233	0.61	1.0	0.59	0.39	97.73	64.09	0.81
	Summer	193	0.24	0.37	0.26	0.13	107.85	52.94	0.39
	Autumn	214	0.26	0.44	0.29	0.18	111.35	67.43	0.44
EMEP	Winter	7	2.61	1.92	1.47	-0.68	56.4	-26.19	2.2
	Spring	18	1.99	1.72	0.69	-0.27	34.75	-13.47	1.05
	Summer	18	0.68	0.69	0.43	0.01	62.25	1.23	0.5
	Autumn	17	1.55	1.15	0.61	-0.4	39.12	-25.94	0.97
EANET	Winter	30	2.11	2.95	2.11	0.84	100.11	39.91	2.86
	Spring	59	1.74	2.67	1.84	0.92	105.65	53.04	2.8
	Summer	59	0.68	0.7	0.72	0.02	105.87	2.38	1.09
	Autumn	59	0.77	1.11	0.77	0.34	99.97	43.4	1.12

Table S2: Seasonal statistical evaluation of EMAC predicted PM_{10} aerosol surface mass concentrations from the Base Case simulation against observations for the period 2008 – 2018.

Network	Season	Number of datasets	Mean Observed (μg m^{-3})	Mean Predicted (μg m^{-3})	MAGE (μg m^{-3})	MB (μg m^{-3})	NME (%)	NMB (%)	RMSE (μg m^{-3})
IMPROVE	Winter	89	7.16	8.36	4.94	1.2	68.9	16.74	6.96
	Spring	222	10.8	7.89	5.48	-2.91	50.77	-26.92	8.64
	Summer	203	14.27	12.85	10.88	-1.42	76.22	-9.98	18.24
	Autumn	207	10.61	6.79	5.45	-3.82	51.33	-35.98	8.67
EMEP	Winter	17	15.2	13.4	6.46	-1.8	42.48	-11.84	7.88
	Spring	34	12.23	10.36	3.8	-1.86	31.06	-15.23	4.98
	Summer	35	12.74	4.92	7.82	-7.82	61.35	-61.35	8.74
	Autumn	36	13.78	8.91	5.13	-4.87	37.21	-35.31	6.22
EANET	Winter	20	38.98	21.49	19.48	-17.49	49.98	-44.87	31.46
	Spring	42	44.52	25.96	20.19	-18.56	45.35	-41.69	27.79
	Summer	41	27.94	9.38	18.56	-18.56	66.43	-66.43	22.73
	Autumn	42	30.43	13.23	17.32	-17.2	56.91	-56.52	21.52

Table S3: Comparison between cloud droplet number concentrations calculated by the Base Case simulation and global observations (Karydis et al., 2017 and references therein).

Location	Latitude	Longitude	Altitude	Time Period	Observed CDNC(cm^{-3})	Simulated CDNC(cm^{-3})
S. Pacific Ocean	20–35˚S	135–175˚W	PBL	Annual	82	146
E. Pacific Ocean	29–32˚N	120–123˚W	450–850 m	July	49–279	136
N. Pacific Ocan	41˚N	131˚W	< 1500 m	April	21–74	166
W. Canary Islands	32˚N	25˚W	PBL	July	17	35
W. Australia	30–40˚S	88–103˚E	PBL	Annual	107	29
Beaufort Sea	72–78˚N	154–159˚W	202–1017 m	June	178–365	14
Beaufort Sea	70.5–73˚N	145–147˚W	300–3000 m	June	20–225	13
Beaufort Sea	65–75˚N	130–170˚W	400–4600 m	April	48–77	30
NE. Alaska Coast	69–71˚N	150–158˚W	400–4000 m	October	10–30	18
Yellow Sea	28–31˚N	127–131˚E	PBL	Annual	30–1000	520
SE Asia Coast	10–40˚N	105–150˚E	PBL	Annual	186 (100–250)	84
N. American Coast	15–35˚N	115–140˚W	PBL	Annual	159 (150–300)	136
S. American Coast	8–28˚S	70–90˚W	PBL	Annual	182 (100–300)	75

S. African Coast	5–25˚S	10–15˚E	PBL	Annual	153 (130–300)	64
NE. Atlantic Ocean	50–55˚N	25–30˚W	800–2200 m	April	65–300	49
Santa Maria, Azores	37˚N	25˚W	550–1000 m	June	150 (74–192)	42
Canary Islands Vicinity	28˚N	16.5˚W	PBL	June – July	51–300	33
W. Moroccan Coast	34˚N	11˚W	PBL	July	77	29
Oregon Coast	45.5˚N	124.5˚W	PBL	August	25–210	216
Key West, FL	24.5˚N	82˚W	PBL	July	268–560	189
Fundy Bay, Nova Scotia	44˚N	66˚W	20–290 m	August	61 (59–97)	182
Cornwall Coast	50˚N	5.5˚W	450–800 m	February	130	112
British Isles, UK	55˚N	2.5˚W	Surface	April	172	126
British Isles, UK	51˚N	6˚W	Surface	October	119	147
British Isles, UK	53˚N	9.5˚W	Surface	December	96	128
SE. England Coast	51.5–52˚N	1.5–2.5˚E	380–750 m	September	151–249	184
SW. Indian Coast	10˚N	65–75˚E	50–550 m	February – March	100–500	280
Qinghai Province	34–37˚N	98–103˚E	PBL	Annual	30–700	219

Beijing	37–41°N	113–120°E	PBL	Annual	30–1100	880
NE. China	39–40°N	117.5 – 118.5°E	1719–1931 m	April – May	200–800	630
Hebei Province	35–40°N	112–119°E	PBL	Annual	30–400	819
Cumbria, England	54.5°N	2.5°W	Surface	March – April	100–2000	123
Cumbria, England	54.5°N	2.5°W	Surface	May	482–549	127
Koblenz, Germany	50°N	7.5°E	901–914 hPa	May	675–900	261
Koblenz, Germany	50°N	7.5°E	945 hPa	October	965	333
N. Finland	68°N	24°E	342–572 m	Annual	154 (30–610)	63
N. Finland	68°N	24°E	342–572 m	October – November	55–470	19
Kuopio, Finland	62.5°N	27.5°E	306 m	August – November	138	89
Cabauw, Netherlands	51°N	4.5°E	PBL	May	180–360	172
Jungfraujoch, Switzerland	46.5°N	7.5°E	Surface	July – August	112–416	204
Barrow, AK	71.5°N	156.5°W	389–830 m	August	56	21
Barrow, AK	71.5°N	156.5°W	431–736 m	May	222	35
Barrow, AK	71.5°N	156.5°W	297–591 m	June	121	23

Barrow, AK	71.5˚N	156.5˚W	393–762 m	July	54	30
Barrow, AK	71.5˚N	156.5˚W	1059–1608 m	September	81	19
Southern Great Plains, OK	36.5˚N	97.5˚W	795–1450 m	Winter	265–281	203
Southern Great Plains, OK	36.5˚N	97.5˚W	343–1241 m	Winter	244	277
Southern Great Plains, OK	36.5˚N	97.5˚W	985–1885 m	Spring	200–219	227
Southern Great Plains, OK	36.5˚N	97.5˚W	671–1475 m	Spring	203	252
Southern Great Plains, OK	36.5˚N	97.5˚W	1280–2200 m	Summer	128–159	648
Southern Great Plains, OK	36.5˚N	97.5˚W	756–1751 m	Summer	131	899
Southern Great Plains, OK	36.5˚N	97.5˚W	1030–1770m	Autumn	217-249	425
Southern Great Plains, OK	36.5˚N	97.5˚W	404–1183 m	Autumn	276	557
Southern Great Plains, OK	36.5˚N	97.5˚W	900–800 hPa	March	200 (100–320)	249
Southern Great Plains, OK	36.5˚N	97.5˚W	300–600 m	April	650	371
Southern Great Plains, OK	36.5˚N	97.5˚W	700–1200 m	September – October	457	717
Cleveland, OH ; Detroit, MI	40–42.5˚N	80.5–85˚W	300–1000 m	August	320–1300	332
Central Ontario	50˚N	85˚W	< 2500 m	October	147 (119–173)	113

Central Ontario	50°N	85°W	2000–2100 m	Summer	350–360	121
Central Ontario	50°N	85°W	1300 m	Winter	190	84
Upper NY State	44°N	75°W	1500 m	Autumn	240	285
State College, PA	41°N	78°W	1000–1600 m	October	388	204
Mount Gibbes, NC	35.5°N	82°W	Surface	Annual	238–754	309
Cape Kennedy, FL	28.5°N	80.5°W	600–2800 m	August	250–330	158

Table S4 : Comparison of estimates for the direct radiative effect (RE_{ari}) of total NO_3^- aerosols from this study and other studies referenced within.

Reference Study	RE_{ari} Estimate (W/m^2)	Time Period
Liao et al., 2004	-0.14	Present Day 2000
Bauer et al., 2007a	-0.11 -0.14	Present Day 2000 Present Day 2030
Bauer et al., 2007b	-0.11	Present Day 2000
Bellouin et al., 2011	-0.12	Present Day 2000
Xu and Penner 2012	-0.12	Present Day 2000
Heald et al., 2014	-0.10	Present Day 2010
This Study	-0.11	Present Day (2008 - 2018)